

## Corrosion protection mechanism of the advanced weathering steel (Fe-3.0Ni-0.40Cu) in a coastal area

Masao Kimura<sup>1)</sup>, Hiroshi Kihira<sup>2)</sup>, Masaharu Nomura<sup>3)</sup>, and Yoshinori Kitajima<sup>3)</sup>

<sup>1)</sup>Adv. Tech. Res. Lab., <sup>2)</sup>Steel Res. Lab., Nippon Steel Corp., <sup>3)</sup> Photon Factory, KEK  
<sup>1)</sup>20-1, Shintomi, Futtsu, Chiba, 293-8511, Japan,

The advanced weathering steel (Fe-3.0Ni-0.40Cu (mass%))<sup>1, 2</sup> shows an excellent corrosion resistance under atmosphere containing air-born salinity. Here we show that advanced weathering steel forms protective rusts which “breath out” chloride ions from rust/steel interface, resulting in a drastic decrease of the corrosion rate by a state-of-the-art nanoscopic mechanism.

Figure 1 compares corrosion properties in a coastal area of advanced and conventional weathering steel; the corrosion amount of the advanced one is less than 1/20 of conventional one after 9-years’ exposure. The rust is composed of inner and outer layers; concentrations of Ni and Na are higher in the inner than the outer layer and Cl shows the opposite trend (Fig.2).

Both inner and outer layers of the rust are composed of  $\alpha$ -FeOOH,  $\beta$ -FeOOH,  $\gamma$ -FeOOH and  $Fe_3O_4$ . The inner layer is composed of fine grains as small as 10-15 nm in radius,<sup>3</sup> and contains  $Fe_3O_4$ . X-ray diffraction (XRD) and X-ray absorption fine structure (XAFS),<sup>4</sup> measurements have shown that nickel atoms substitute Fe-sites of  $Fe_3O_4$  to form  $Fe_{3-x}Ni_xO_4$  (Fig.3).

Good corrosion resistance of the advanced weathering steel can be attributed to fine grain-size distributions of the inner layers and the formation of  $Fe_{3-x}Ni_xO_4$  (Fig.4). When atmospheric corrosion progresses in a wet condition, its pH becomes low because of hydrolysis. In conventional weathering steel, the rust made of only FeOOH is positively charged by attached H<sup>+</sup> ions. However, the inner rust of advanced weathering steel contains  $Fe_{3-x}Ni_xO_4$  and is negatively charged. The rusts “breath out” chloride ions from rust/steel interface.<sup>5</sup>

<sup>1</sup> H. Kihira, A. Usami, K. Tanabe, M. Ito, G. Sigesato, Y. Tomita, T. Kusunoki, T. Tsuzuki, S. Ito, and T. Murata, in *Symp. on Corrosion and Corrosion Control in Saltwater Environments (Joint Int. Meeting of the Electrochemical Soc. and the Electrochemical Soc. of Japan)*, edited by D. A. Shifler, T. Tsuru, P. M. Natishan and S. Ito (The Electrochemical Soc. Inc., Honolulu, 1999), p. 127.

<sup>2</sup> H. Kihira, S. Ito, T. Mizoguchi, T. Murata, A. Usami, and K. Tanabe, *Zairyo-to-Kankyo* 49, 30 (2000).

<sup>3</sup> Y. Ishii, M. Kimura, H. Kihira, and T. Mizoguchi, in *205th Meeting of The Electrochemical Society*, Orland, FL, 2003.

<sup>4</sup> B. K. Teo, *EXAFS: Basic Principles and Data Analysis*

(Springer, Berlin, 1986).

<sup>5</sup> M. Kimura, H. Kihira, Y. Ishii, and T. Mizoguchi, in *13th Asian-Pacific Corrosion Control Conference*, Osaka, 2003.

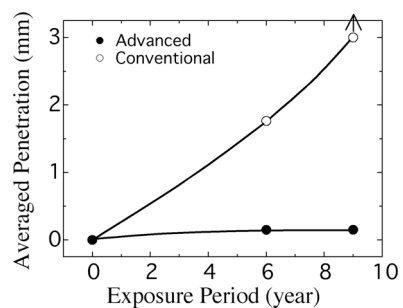


Figure 1 Penetration curves of advanced and conventional weathering steel exposed to marine atmosphere.



Figure 2 Compositional mapping of the cross-section of the rust in a black (high concentration) - white scale.

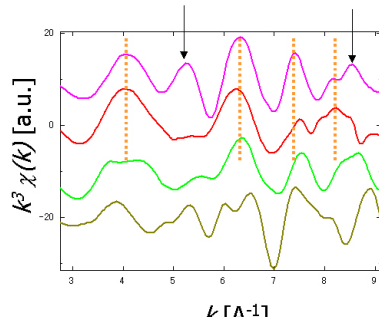


Figure 3 XAFS spectra in the form of  $k^3\chi(k)$ , where  $k$  is the wave number and  $\chi(k)$  is the oscillation term: NiO at Ni K-edge (bottom),  $\alpha$ -FeOOH at Fe K-edge, the inner layer at Ni K-edge,  $Fe_3O_4$  at Fe K-edge (top). Some of the spectra were shifted along the x-axis for comparison.

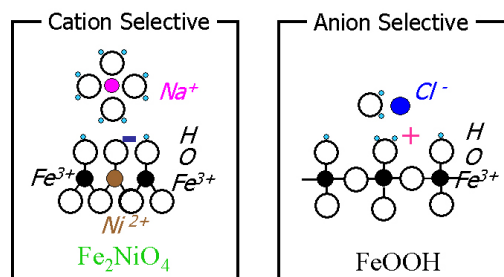


Fig. 4 Schematic diagram of the interface between a rust and a solution on it, when pH of the solution is low.